Posprint of: Journal of Photochemistry and Photobiology A: Chemistry, Volume 223, Issue 1, 5 September 2011, Pages 25–36

Self-association of a naphthalene-capped-β-cyclodextrin through cooperative strong hydrophobic interactions

M. José González-Álvarez (a), Alejandro Méndez-Ardoy (b), Juan M. Benito (c), José M. García Fernández (c), Francisco Mendicuti (a)

(a) Dpto. Química Física, Universidad de Alcalá, Edificio de Farmacia, Campus Universitario Ctra. Madrid-Barcelona Km 33,600, E-28871 Alcalá de Henares, Madrid, Spain

(b) Dpto. Química Orgánica, Universidad de Sevilla, Fac. de Química, E-41012 Sevilla, Spain

(c) Instituto de Investigaciones Químicas, CSIC–Universidad de Sevilla, E-41092 Sevilla, Spain

Abstract

NMR, circular dichroism and fluorescence techniques were used to study the structure in solution of a new β-cyclodextrin derivate in which naphthalene chromophore group is bridged to O(2) and O(3) secondary positions of the same glucopyranose unit through a bidentate hinge. The results point to the formation of a very stable dimer in aqueous solution which dissociates in non-polar solvents. Dimerization was enthalpy and entropy favoured. The hydrophobic character of the naphthyl moiety plays a very important role in the entropy change sign. Molecular mechanics as well as molecular dynamics calculations indicated that the most stable dimers are head-to-head oriented. For these dimer structures the naphthyl moieties, relatively shielded from the solvent, are sufficiently close to each other to couple their transition moments, but without forming excimers.

Highlights

► Dimerization processes, structure and conformational behavior of a new naphthalene-β-cyclodextrin derivate. ► A wide variety of experimental techniques (NMR, UV-absorption, steady-state and lifetime fluorescence and circular dichroism) was used. ► CD derivative self-assemble by strong hydrophobic interactions without the need for inclusion in the neighbor CD. ► Dimerization was enthalpy and entropy favoured. ► Molecular modelling indicated dimers are head-to-head oriented.

Keywords

Cyclodextrins; Fluorescence; Circular dichroism; Molecular modelling; Hydrophobic effect

1. Introduction

Cyclodextrins (CDs) are cyclic oligosaccharides composed of 6, 7 or 8 d-glucopyranose termed α, β and γCD, respectively. Because of their hydrophobic cavity, they are capable of forming

inclusion complexes in water with a great variety of organic compounds [1] and [2], which makes them ideal for many supramolecular applications including drug delivery, sensors or molecular machines [2] and [3]. The utility of native CDs is often limited because of their relatively low discrimination character among guests of similar size, solubility, which is restricted to water or very polar solvents [4], and the conformational constrains imposed by the cyclooligosaccharide architecture. Efforts have been made to chemically modify natural CDs in order to manipulate their binding properties, enhance the enantioselectivity towards chiral guests, achieve solubility in a desired solvent or investigate the inclusion mechanism [5]. In this context, O-methylated CDs offer many advantageous features for applications in fields such as the separation of chiral molecules or drug encapsulation [6]. Thus, permethylated CDs exhibit a larger flexibility as compared to the native CDs, with a wider cavity and higher solubility in both aqueous and organic solvents [7], [8] and [9].

Fluorescently labeled CD derivatives represent very useful tool for sensing applications and supramolecular studies. The attachment of a chromophore to a CD not only alters the original binding ability and selectivity, but also provides a spectroscopic probe for investigating the structure, conformations and the molecular recognition of multiple molecules [10], [11], [12] and [13]. The naphthalene group is particularly attractive for this purpose due to the numerous applications in photochemical molecular devices [14] and fluorescence molecular sensors [14], [15], [16], [17], [18], [19] and [20]. Consequently, a great effort has been devoted to investigate the structure, conformation and aggregation properties in solution of naphthalene-modified CDs. Ueno et al. [21] and [22] have studied the self-inclusion processes of βCD bearing two naphthyl moieties linked to the primary CD face. One of the two pendant naphthyl moieties seems to move outwards–inwards from the inner cavity. Equilibrium is reached between a predominant form in which a naphthyl group is included into the CD cavity and another one where both naphthyl groups are located outside. The conformational changes in the appended group, which were monitored by excimer fluorescence and circular dichroism, were guest-dependent. Valeur's group [23], [24] and [25] have reported the photophysical properties of βCDs bearing several 2-naphthoyloxy chromophores substituted at one or both CD faces. These systems were used as a model for studying the excitation energy transfer process among naphthalene moieties. Garcia-Garibay and McAlpine [16], [26] and [27] described the synthesis and the inside-outside isomerism of 3-O-(2-methylnaphthyl)-βCD. 1H NMR experiments revealed the presence of dimers at concentrations higher than 0.1 mM. The circular dichroism spectrum of diluted samples was, however, consistent with a monomer form. 1H NMR chemical shift variations as a function of concentration provided a monomer–dimer equilibrium constant of 5000 M−1 at 25 °C [16]. Other authors [17] and [18] have studied how the differences in the chain length of the linker of the appended naphthyl group to the CD affect the association behaviour of the modified βCD. The presence of dimers for the 6-O-mono-2-naphthoate βCD, where the 2-naphthoyl moiety is directly attached to the CD, was demonstrated. However, when the chromophore group is connected to the CD through a relatively long chain as in 6-[(N-2-naphthoyl-2-aminoethyl)amino]-6-deoxy βCD the molecule prefers to adopt a self-inclusion conformation. Park et al. have also synthesized CD derivates bearing different chromophoric moieties [15], [19] and [20], among which the 6-O-(2-sulfonate-6-naphtyl)-βCD. This compound exhibits a monomer–dimer equilibrium with a high dimerization constant (∼104 M−1 at 25 °C) [28] and [29]. The naphthyl group did not present

an excimer band in the fluorescence spectra but it did show an exciton coupling band in the circular dichroism spectrum which denotes a relative proximity between naphthyl moieties. More recently, Liu et al. [11] have reported the synthesis of two novel permethylated βCD derivates containing naphthalene and quinoline appended groups. The results from circular dichroism and ROESY spectra showed that both chromophores are deeply self-included into the cavity of the CD. Nevertheless, both groups are expelled towards the narrow primary face upon complexation of bile salt guests.

A common characteristic of the above commented works is that the chromophore substituent is linked to a single glucopyranose position at either the primary or the secondary rim. The conformational and aggregation properties in solution are then dictated by the ability to form intra- or intermolecular inclusion complexes. However, we have reported the self-association processes of 2I,3I-O-(o-xylylene)-permethylated CDs (XmCD) in which a xylylene chromophore group bridged simultaneously vicinal O(2) and O(3) of the same glucopyranose [30], [31] and [32]. Small dimerization equilibrium constants were obtained (KD: ∼180, ∼200 and 248 M−1 for Xmα-, -β- and -γCDs, respectively, at 25 °C). Dimerization processes were accompanied by $\Delta H < 0$ and $\Delta S < 0$. Molecular dynamics simulations for XmCD monomers demonstrated the presence of an open (or half-open)/capped equilibrium which is significantly displaced to the open conformation. Calculations also revealed that the most stable dimers are those formed when two XmCDs approach through their secondary faces (head-to-head, HH).

In addition, the XmCDs shows negative solubility coefficients in water, being more soluble in cold than in hot water. This situation is analogous at that observed for per-O-methylated and partially methylated CD derivatives [33]. X-ray studies in this series suggest that the reverse solubility as compared with canonic CDs is due to the breakdown of hydration networks leading to aggregation [34], [35], [36], [37], [38], [39], [40] and [41]. Although this particular behaviour can be attributed, in essence, to the hydrophobic effect, the crystallographic studies alone do not allow determining the pathway which leads from high solubility in cold water to low solubility at higher temperature. The presence of the doubly linked aromatic ring in XmCDs seems to exacerbate this effect, favouring the formation of well-defined dimeric species in solution through a mechanism that does not involve inclusion phenomena. These modified CDs may thus serve as well-defined systems to study the hydrophobic effect in more deep by using spectroscopic techniques.

This work describes the synthesis and study the behaviour in water of a hinge-type capped CD named 2I,3I-O-(1,8-naphtylene)-per-O-Me-β-cyclodextrin (NmβCD), which contains a naphthyl cap-like moiety. Dimerization equilibrium constant, thermodynamic parameters upon association and information about the structure in water were obtained by using NMR, fluorescence, circular dichroism and molecular modelling techniques. The complexation of 1,8-dimethoxynaphatalene (oN) [42] and the hetero-association of NmβCD both with heptakis(2,3,6,-tri-O-methyl)βCD (MeβCD) were also studied.

To the best of our knowledge, this is the first report on a naphthyl appended CD derivative that self-aggregates by strong hydrophobic interactions with really large binding constants and without the need for inclusion of the substituent into the partner CD. Compared to βCD derivatives bearing a single-linked naphtyl substituent, the double-linked hinge-type

disposition should impose significant conformational constraints. Notably, it forces a quasi-perpendicular disposition of the major axis on the naphthalene moiety and the central axis of the βCD molecule, disfavouring self-inclusion and/or penetration into the partner CD.

2. Experimental

2.1. Synthesis and characterization

Briefly, the synthesis of 2I,3I-O-(1,8-naphtylene)-per-O-Me-β-cyclodextrin (NmβCD), was accomplished in two steps starting from its xylylene-appended counterpart XmβCD [30] (Scheme 1). Catalytic hydrogenation of the benzylic ether furnished the selectively differentiated vicinal diol diOHmβCD which can be now reacted with an excess of 1,8-bis(bromomethyl)naphthalene in DMF in the presence of sodium hydride (Scheme 1). One-pot double alkylation furnished the target compound NmβCD (37% overall yield from XmβCD). The structures of the diOHmβCD intermediate and NmβCD were confirmed by NMR, electrospray mass spectra (ESIMS) and combustion analysis. Synthetic details as well as characterization data are included in Supporting Information (Figs. S4–S6).

2.2. Solution preparations, instruments and experimental details

The solutions of NmβCD used for fluorescence and circular dichroism experiments were prepared by weight in deionized water (Milli-Q) and stirred for ∼24 h prior to measuring. The concentrations ranged from 0.002 to 0.4 mM. For the aqueous solution of MeβCD the concentration range was wider reaching concentrations close to 11 mM. All the organic solvents used in the fluorescence and circular dichroism experiments were spectroscopic or purity > 98% grades. Nevertheless they were always checked before use. 2,3-Butanedione (diacetyl, Aldrich) was used as fluorescence quencher for the naphthyl group. Sodium 1-adamantanecarboxylate (AC) and/or adamantyl-1-amine (AA) were also used as control guest molecules to probe the accessibility to the βCD cavity in water. 1,8-Bis(methoxymethyl)naphthalene (oN) was prepared as previously described from the corresponding 1,8-bis(hydroxymethyl) naphthalene [43].

1H NMR, 2D COSY, 1D NOESY and 1D TOCSY experiments were performed by using a 500 MHz, Bruker 500 DRX instrument in the 5–60 °C temperature range. For NMR measurements solutions of NmβCD in deuterated water were prepared in the 1.42–22 mM range. Though the lowest concentration was still above the detection limit for this particular compound, no significant spectral changes were observed by working below 1 mM. For NMR titration experiments, 1.5 mM stock solutions of NmβCD in D2O were prepared. A 500-μL aliquot of the stock solution was transferred to a 5-mm NMR tube, and the initial NMR spectrum was recorded. A solution (10–20 mM) of the guest (AC or AA) in the previous stock solution of NmβCD was then prepared. Aliquots of this solution were gradually added to the NMR tube via microsyringe, recording the corresponding spectrum after each addition. Additions were continued until complete saturation of the host. Chemical shift variation of the host diagnostic signals were plotted against the guest concentration and binding constants were calculated from these data by using a least-squares fitting protocol [42].

Steady-state fluorescence was performed by using a high sensitivity spectrofluorimeter, the SLM 8100C Aminco, equipped with a cooled photomultiplier and a double (single) monochromator in the excitation (emission) path. The fluorescence decay measurements were achieved on a time correlated single photon counting (TCSPC) FL900 Edinburgh Instruments Spectrometer with a thyratron-gated lamp filled with H2. Circular dichroism (ICD) spectra were obtained by using a JASCO-715 spectropolarimeter (see Supporting Information, Instruments and Experimental Details).

3. Results and discussion

3.1. Absorption spectra

As depicted in Fig. 1, the NmβCD absorption spectrum in water exhibits two intense main bands whose maxima are placed at 220 and 290 nm and a very faint one located at 320 nm. NmβCD/water solutions show spectra that very well match the one observed for the oN model compound but whose maxima are slightly shifted to the blue by about 4 nm. By comparison the of oN structure with similar naphthalene derivates [44] and [45], these bands can be ascribed, according to Platt's notation [46], to the 1Bb, 1La and 1Lb electronic transitions. For these transitions dipole moments (superimposed in Fig. 1) are nearly parallel to the long (1Bb) and short (both 1La and 1Lb) naphthalene main axis.

3.2. Fluorescence measurements

3.2.1. Emission spectra

Fig. 2 shows the emission spectra for NmβCD/water solutions upon excitation of the naphthyl group at 295 nm. Each spectrum exhibits a double band located at ∼335 and ∼342 nm and a shoulder at ∼355 nm. The fluorescence intensity obviously increases upon increasing the NmβCD concentration, but this fact does not affect the ratio between the intensities of the two main bands. This, in addition to the fact that the spectra never showed a broadening to the red, denotes the absence of any intermolecular naphthalene excimers.

The association constant KD for the dimerization process of NmβCD described by the equilibrium:

$$2\,\mathrm{N}m\beta\mathrm{CD} \rightleftarrows (\mathrm{N}m\beta\mathrm{CD})_2$$

can be related with the fluorescence intensity (I) measured as the area under the naphthyl group emission spectrum, and the total NmβCD concentration by Eq. (2)[31]:

$$I = \phi_{(\mathrm{N}m\beta\mathrm{CD})_2}[\mathrm{N}m\beta\mathrm{CD}]_0 - \left(\phi_{(\mathrm{N}m\beta\mathrm{CD})_2} - \phi_{\mathrm{N}m\beta\mathrm{CD}}\right)\frac{\left(\sqrt{8K_\mathrm{D}[\mathrm{N}m\beta\mathrm{CD}]_0 + 1} - 1\right)}{4K_\mathrm{D}}$$

where φ(NmβCD) and $\phi_{(\mathrm{N}m\beta\mathrm{CD})_2}$ are the proportionality constants (per chromophore unit) between fluorescence intensity and concentration of the monomer and dimer forms.

A plot of the corrected fluorescence intensity taking into account the inner effect, (Icorr) with [NmβCD]0 at 25 °C is inserted in Fig. 2 (more details in Instruments and Experimental Details in Supporting Information). This representation is linear and the Icorr/[[NmβCD]0 ratio remains constant in the whole range of NmβCD concentrations used in our measurements. This fact demonstrates, according to Eq. (2), that $\phi_{(\mathrm{Nm\beta CD})_2} \cong \phi_{\mathrm{Nm\beta CD}}$ or in other words, the fluorescence quantum yield does not change with the dimerization process.

3.2.2. Fluorescence intensity decays

Time-resolved fluorescence measurements for NmβCD aqueous solutions at different concentrations and temperatures were performed at the maximum of the emission band (342 nm) upon excitation of the naphthyl group (295 nm).

The fluorescence intensity decay profiles were fitted to three-exponentials at any [NmβCD] and temperature [47]. The short lived component (~0.2 ns) was ascribed to the innate stray light and/or scattering of the cylindrical cuvettes used. The intermediate (~12 ns) and the slowest (~30 ns) components were assigned to the free (NmβCD) and the dimer (NmβCD)2 species, respectively.

As shown in Fig. 3, the fractional contribution of the intermediate component decay time, fNmβCD, (more details in Instruments and Experimental Details in Supporting Information), decreases with [NmβCD], whereas the contribution of the slowest component, $f_{(\mathrm{Nm\beta CD})_2}$, increases and, in agreement with an enthalpy-favoured association process, it noticeably decreases with temperature due to complex dissociation. In consequence, the weighted average lifetimes $\langle\tau\rangle$ defined as:

$$\langle\tau\rangle = f_{\mathrm{Nm\beta CD}}\tau_{\mathrm{Nm\beta CD}} + f_{(\mathrm{Nm\beta CD})_2}\tau_{(\mathrm{Nm\beta CD})_2}$$

where τNmβCD and $\tau_{(\mathrm{Nm\beta CD})_2}$ are the lifetimes for both species, increase (decreases) with [NmβCD] (temperature) as inferred from Fig. 3.

3.2.3. Thermodynamics of the dimerization processes

The variation of the average lifetime ($\langle\tau\rangle$) against [NmβCD]0 at different temperatures is depicted in Fig. 4. The $\langle\tau\rangle$ increasing with [NmβCD]0 is due to the increase in the dimer fraction. The near plateau is achieved at very low concentrations pointing towards a high dimerization constant.

Additionally, these experimental data can be fit to the following non-linear equation [31]:

$$\langle\tau\rangle = \frac{2\tau_{\mathrm{Nm\beta CD}} + (\phi_{(\mathrm{Nm\beta CD})_2}/\phi_{\mathrm{Nm\beta CD}})\,\tau_{(\mathrm{Nm\beta CD})_2}\left(\sqrt{8K_{\mathrm{D}}[\mathrm{Nm\beta CD}]_0 + 1} - 1\right)}{2 + (\phi_{(\mathrm{Nm\beta CD})_2}/\phi_{\mathrm{Nm\beta CD}})\left(\sqrt{8K_{\mathrm{D}}[\mathrm{Nm\beta CD}]_0 + 1} - 1\right)}$$

The experimental data which fit reasonably to the curve generated by Eq. (4) under the assumption that $\phi_{(\mathrm{Nm\beta CD})_2}/\phi_{\mathrm{Nm\beta CD}} = 1$, provide association constants at different temperatures collected in Table 1. The KD values obtained were significantly high in

comparison with those calculated for similar naphthalene-substituted βCDs [16], [17], [18], [28] and [29].

The thermodynamic parameters for the dimerization process were attained from the van't Hoff linear representations (Fig. S1 in Supporting Information). Both ΔH (−21.3 ± 2.7 kJ mol−1) and ΔS (+24.7 ± 9.2 J K−1 mol−1) parameters favour NmβCD dimerization. Intermolecular CD associations by attractive van der Waals or electrostatic interactions are usually characterized by ΔH < 0. In fact, the value and sign of ΔH is very similar to that obtained for the dimerization process of XmβCD (and their XmαCD and XmγCD partners [31] and [32]) and also for the complexation of many other naphthalene derivates with βCDs [48], [49], [50] and [51]. The favourable positive value of ΔS for NmβCD, in contrast with the negative value found for XmβCD (and also for XmαCD and XmγCD [31] and [32]), must be due to the different size of the appended moiety and the higher hydrophobicity of a naphthyl group in aqueous medium, as compared to the benzyl group. For a dimerization process, the quantitative value and sign for ΔS is the result of the balance between two opposite factors: (i) the expected loss of degrees of freedom accompanying any self-assembling and (ii) the reorganization of host and guest solvating water molecules during the process [52]. The larger size of the naphthalene compared to the benzene, will cause a larger loss of solvating shells during NmβCD dimerization and consequently this effect will contribute more favourably to ΔS.

3.2.4. Fluorescence quenching

The fluorescence quenching experiments are quite useful to determine the accessibility of a free quencher to the naphthyl anchored to the βCD, giving information about its location. Quenching measurements by diacetyl were carried out on oN (very diluted) and NmβCD/water solutions at 25 °C. For the latter system two NmβCD concentrations (2.68 × 10−3 mM and 0.257 mM) were employed. At these concentrations and temperature the dimer molar fractions were approximately 0.15 and 0.8, respectively. Stern–Volmer $\langle\tau 0\rangle/\langle\tau\rangle$ plots were linear in the whole range of concentrations used. The Stern–Volmer constants (KSV) were 40.9, 26.9 and 2.5 M−1 for oN and 2.68 × 10−3 mM and 0.257 mM NmβCD, respectively. The bimolecular quenching constants (kq) [53] for each system were (3.0 ± 0.2) × 109, (1.6 ± 0.5) × 109 and (8.5 ± 0.6) × 107 M−1 s−1, respectively. These results demonstrate that naphthyl moiety in the isolated oN is obviously much more accessible to the quencher than in the NmβCD dimer, where it is probably shielded by the two CD macrorings (or perhaps partially included into the partner CD). As expected, kq values drastically decreases with the dimer fraction. In addition, the temperature dependence on kq was obtained for the 0.257 mM NmβCD/water solution. kq's of (3.7 ± 0.2) × 107, (8.5 ± 0.6) × 107 and (1.9 ± 0.2) × 108 M−1 s−1 for 5 °C, 25 °C and 45 °C, respectively, were in agreement with ΔH < 0.

3.2.5. Dependence of the fluorescence quantum yield and lifetime with medium polarity (ε) and microviscosity (η)

The influence of the medium ε and η on the fluorescence quantum yield (Φ) and lifetime (τ) for the naphthyl moiety in NmβCD was assessed by measuring dilute solutions of the oN model in several solvents (water, methanol/water, ethanol/water mixtures and n-alcohols) at 25 °C. The results (Fig. S2, Supporting Information) reveal that in the case of the oN derivative τ decreases

with ε, for ε > 50, and it increases with η. Φ, however, does not show any special trend when varying ε and η (Φ ≈ 0.08 ± 0.06). Dimer formation in NmβCD may involve a decreasing (increasing) in polarity (microviscosity) surrounding the chromophore (appended naphthyl placed between both CDs or perhaps included in the inner cavity of a βCD partner whose ε ≈ 50 [32]). These results may therefore agree with τ(NmβCD)2>τNmβCD and with τ(NmβCD)2>τNmβCD and with φ(NmβCD)2≅φNmβCD.

Fluorescence decay measurements on NmβCD solutions in different polarity solvents were also performed. The concentrations used were similar in all experiments, [NmβCD] ≈ 0.2 mM (dimer molar fraction ∼0.8). Fig. 5 depicts the ratio of the fractional contributions for decay times attributed to the dimer and monomer species and $\langle\tau\rangle$ variations with ε. Results indicate a decrease in both the fractional ratio values and $\langle\tau\rangle$ when decreasing the solvent polarity as a consequence of the dissociation of the (NmβCD)2 into the monomer species with a faster lifetime component.

On the other hand, it is well known the large affinity of adamantane derivatives for βCD by forming 1:1 strong stable complexes (K ∼ 104 M−1) in water [12], [54], [55] and [56]. Processes like self-inclusion of CD appended groups, dimer formation or any other guest complexation may compete with this strong complexation. Sodium 1-adamantanecarboxylate (AC) was added to each of the previously studied NmβCD (0.2 mM) solutions up to reaching [AC] = 1.6 mM (8-fold excess). Results are also represented in Fig. 5 and show that the addition of excess AC does not produce any significant changes neither in $\langle\tau\rangle$, nor in the fractional dimer-to-monomer contribution ratios whatever the polarity of the solvent was.

3.3. Circular dichroism measurements

The magnitude and sign of the ICD spectrum of a chromophore guest when it interacts with a CD can inform about its location with respect to the CD [57], [58], [59], [60] and [61]. The ICD spectrum sign varies depending on the type and depth of the guest inclusion in the CD cavity and the orientation of its electronic transition moment relative to the CD n-fold axis. Parallel (perpendicular) orientation gives a positive (negative) ICD band which becomes opposite sign when the chromophore is located partially outside [57], [58], [59], [60] and [61].

Fig. 6 (upper) shows the circular dichroism spectrum of NmβCD (0.2 mM in water) at 25 °C. At this concentration and temperature around the 80% of the NmβCD is in dimer form. The ICD spectrum exhibits a relatively intense exciton coupling (EC) band in the electronic 1Bb transition region, whereas a slightly positive band is observed in the 1La zone. ICD spectrum for EC is characterized by the typical bisignate Cotton effect that takes place when two chromophores are close enough to couple their electric transition moments. In general, stronger absorption and smaller interchormophore distances leads to larger intensity for the positive and negative peaks in the EC signal [62]. In case of a pair of naphthalene moieties, EC takes place when they are spaced out by around 7 Å [62]. Thus, EC signal observed for the 1Bb band in water most probably points towards the presence of HH-type (NmβCD)2 dimers in this solvent. Furthermore, this structure would be presumably stabilized through mutual

cooperative interactions between the naphthyl groups, or even between naphthyl groups and secondary methyl groups, as predicted before for (XmCD)2 dimers [30], [31] and [32].

Different polarity solvent-induced circular dichroism variations on NmβCD were also examined and depicted in the bottom panel of Fig. 6. Variations in the solvent polarity (the same solvents and concentrations as in the previous section) made drastic changes in the ICD spectra band shape and intensities. Whereas the 1La intensity band monotonically decreases when decreasing medium polarity (ε), the intensity of the EC dual band decreases down to methanol, and then, becomes a single positive band in less polar solvents. This means that when the medium surrounding NmβCD becomes more and more hydrophobic, the interaction between naphthyl groups turns weaker, shifting the equilibrium towards the monomeric species. The relatively intense positive 1Bb and weak 1La bands in the non-polar solvents would agree with a monomer NmβCD species where the naphthyl group, interacting with its CD macroring, would be located outside the cavity and lying relatively parallel to it, according to Kodaka's rules [57] and [59]. Similar conclusions were reached from lifetime measurements described earlier in this paper, where a decrease in medium polarity means an increase in the monomer fraction. These would also agree with the explanation given for the $\Delta S > 0$ for NmβCD dimerization in water, where the hydrophobic effect is assumed to play an important role.

As with fluorescence measurements, neither the intensity nor the shape at the 1Bb or 1La ICD bands were influenced by the addition of AC to the NmβCD solutions used in our previous experiments at 25 °C. Complexation of AC with NmβCD in polar solvents cannot compete with its strong self-association at 25 °C. Same behaviour was observed at 45 °C in water. Furthermore, the results also reflect that AC does not form inclusion complexes with NmβCD in non-polar solvents. Similar conclusions were reached from time-resolved measurements at 25 °C (or 45 °C).

The variation of the ICD with the concentration for NmβCD/water solutions for the 1La band at 25 °C was also studied. Unfortunately, due to the low absorptivity of this band, it was not possible to get reliable ICD signals at concentrations smaller than 0.25 mM. For NmβCD concentrations larger than 0.25 mM only a slight variation in the ICD signal with [NmβCD] is observed, since the plateau, as shown in Fig. 4, is almost reached. Even so, the experimental data can reasonably be adjusted to a non-linear equation similar to Eq. (3), by using the KD value obtained previously by fluorescence lifetime measurements at the same temperature [63].

3.4. Study of the heterodimerization process

To evaluate the role of the naphthyl moiety in the intermolecular self-association of NmβCD, the heterodimerization between NmβCD and permethylated βCD (MeβCD) at different temperatures was also studied. The results show a fairly small decrease in $\langle\tau\rangle$ with [MeβCD]. At the [NmβCD] used, ~80% of NmβCD forms a very stable dimer, and even the addition of a great excess of MeβCD (up to ×70 times) does not force (NmβCD)2 to dissociate, i.e. does not substantially decrease $\langle\tau\rangle$. These results reinforce the idea that the mutual and strong cooperation between naphthyl groups is mainly responsible for the high (NmβCD)2 stability. The study of the oN model complexation with MeβCD was also tackled. $\langle\tau\rangle$ for oN/MeβCD

water solutions ([oN] kept constant) also hardly change upon MeβCD addition at any temperature. oN nearly does not interact with MeβCD or if it does, its binding constant is extremely low (Fig. S3 in the Supporting Information).

These experiments demonstrate that two interacting naphthyl groups are required to make a presumably HH-type dimer formation possible. It also supports that this interaction does not involve inclusion of the naphthalene moieties in the CD cavities. Circular dichroism also reinforces this fact. In both the NmβCD/MeβCD and oN/MeβCD experiments, the ICD spectra did not exhibit any variation with [MeβCD] either.

3.5. NMR measurements

In contrast to that reported for the analogous xylylene-tethered βCD counterpart [47], [48], [49], [50], [51] and [52], 1H NMR spectra for NmβCD in D2O at different concentrations (1.42–22 mM) and temperatures (5–50 °C) featured no significant proton chemical shift variations (see Fig. S7, Supporting Information). This observation fits with the remarkably high dimerization constant (KD) determined by time-resolved fluorescence. In fact, the NmβCD concentrations used in NMR experiments exceed the concentrations at which, according to Fig. 4, any chemical shift variations must be observed. The scenario is similar to that encountered when ICD signal variation with [NmβCD] for the 1La band was monitored.

The remarkable 1H NMR spectrum signal splitting observed for NmβCD in D2O solutions at 25 °C is ascribable to the large anisotropic effect induced by the naphthyl group and further supports that the naphthalene moiety is relatively close to the secondary rim of the CD torus in the dimer, so that all glucose protons become affected by the associated electronic current. Full assignment of the seven magnetically non-equivalent glucopyranosyl units was then possible by combining 2D COSY and 1D TOCSY experiments (Fig. S8, Supporting Information). The observation of cross-peaks in the NOE spectra between aromatic protons and methoxy groups at the secondary rim of the CD moiety (Fig. S9, Supporting Information) is also in agreement with the HH orientation of the two CD partners upon dimer formation.

Extensive precipitation occurred in D2O solutions of NmβCD above 50–60 °C (depending on the concentration) resulting in line broadening in the NMR spectra, which probably indicates that the monomeric species, whose fraction increases with temperature ($\Delta H < 0$), is too insoluble in D2O to allow detection by NMR.

The shape of the 1H NMR spectrum for NmβCD collected in deuterated chloroform (1.5 mM at 25 °C) was sharply different to that registered in D2O, with extensive overlapping of the signals, indicating that the naphthalene ring is probably more distant from the CD cavity and exposed to the solvent. The spectrum did not change with concentration or temperature, and no precipitation was observed. This agrees with the conclusions inferred from the fluorescence and ICD experiments indicating that monomeric species are mainly present in non-polar solvents.

The capability of NmβCD to form inclusion complexes in water with either adamantane-1-carboxilate (AC) or adamantyl-1-amine (AA) was also assayed by NMR. Virtually no changes on

the proton chemical shifts of NmβCD were observed upon titration with either of the guests up to 10-fold molar excess, which denotes that complexation of AC or AA with NmβCD does not take place. This is sharply different to that previously observed for XmβCD or the permethylated βCD (MeβCD), which formed 1:1 complexes with AC (binding constants of 443 ± 2 M−1 and 965 ± 15 M−1, respectively, at 25 °C) [30]. This observation further supports the existence of an aggregate stabilized through hydrophobic interactions at relatively low temperatures, in which the access to the cavity is blocked.

3.6. Molecular mechanics and molecular dynamics calculations

Molecular mechanics (MM) and molecular dynamics (MD) calculations were performed with Sybyl 8.0 [64] and the Tripos Force Field [65]. A relative permittivity ε = 3.5 (ε = 1) was used in the vacuum (in the presence of water). Charges for NmβCD were obtained by MOPAC [66]. The starting NmβCD were built with the macroring in the non-distorted form (φ = 0° and ψ = −3°, τ = 121.7° and side chain χ angles in the trans conformation [67]) and the naphthyl substituent in some of the most probable conformations (ten) for the chain that links the naphthalene moiety to a glucopyranose unit of the βCD macroring. These ten selected conformations for NmβCD appended group were those of the minima potential energies (MBE) from a total of 400 starting conformations obtained by placement of the four torsional angles that describe the rotation around C(3)–O–CH2–Car(1) and C(2)–O–CH2–Car(8) ether bonds at the maxima of their probability distribution functions and further structures minimization. These distributions (depicted in Fig. S10, Supporting Information) were obtained from the analysis of the 10 ns MD trajectories (at 600 K) performed on an isolated glucopyranose linear trimer, where the central unit contains the bidentate naphthalene moiety substituted at the C(2) and C(3) positions (a description of the method is included in Supporting Information, page 21). Structure optimizations were carried out by the simplex algorithm, and the conjugate gradient was used as a termination method with gradients of 0.2 (0.5) kcal mol−1 Å−1 for the calculations carried out in vacuum (water) [68] and [69]. Non-bonded cut-off distances were set at 8 Å. For calculations in water the Molecular Silverware algorithm (MS) [70] was used for solvation with periodic boundary conditions (PBC) in a canonical (NTV) ensemble.

The methods used for (i) the conformational study of the isolated NmβCD structures and (ii) the dimer (NmβCD)2 formation were similar to those described previously [31] and [32]. (i) For the isolated NmβCD, 5 ns MD simulations in the vacuum were made at several temperatures ranging from 350 to 600 K on each of the (10) initial NmβCD structures (Supporting Information, Fig. S11 and page 21). For these structures, in contrast with XmβCD which contain a xylylene moiety [31] and [32], the bulkier naphthyl moiety characteristics and its substitution at the 1 and 8 naphthalene positions, only make two, full-open and open, conformations possible. Those capped conformations which appeared in XmβCD, for NmβCD are excluded [31] and [32]. (ii) Dimerization processes were performed starting from the minimized most stable full-open and open (Supporting Information, named 1 and 2, Fig. S11) NmβCD structures by considering three different CD-to-CD approaching, named HH, HT and TT-type (H = head; T = tail) (coordinate system to describe the approaching during dimerization process is depicted in Fig. S11). Critical analysis of the structures generated by scanning the θ [O(4)–o–o'–O(4')] dihedral angle in the −180 to 180° range (10° intervals), the ε [o–o'–O(4')] angle from 50 to 130° (10° intervals) and the y coordinate (oo' distance) from 20 to 6 Å (1 Å intervals) in the

vacuum, followed by optimization (0.2 kcal mol−1 Å−1) provided the most favourable θ and ε angles for approaching. Initially fixed these θ and ε angles at those values, the dimerization was emulated by approaching in 0.5 Å steps along the y coordinate from 20 to 6 Å now in the presence of water (MS, PBC, NVT). Every structure was optimized (1.0 kcal mol−1 Å−1) and saved for further analysis. Minima binding energy (MBE) structures for dimers were optimized once again (0.5 kcal mol−1 Å−1) and used as the starting conformations for the 1.0 ns MD simulations following the same strategy described earlier (Supporting Information, page 21) [31] and [32].

3.6.1. Conformational study of NmβCD

Probability distribution for φi and ψi torsional angles of the NmβCD macroring was obtained from the analysis of the 10 ns molecular dynamics trajectories in the vacuum at different temperatures on ten most stable structures for NmβCD (Fig. S11, Supporting Information). These structures were full-open or open. The φi and ψi angles for these structures like to adopt two typical skewing conformations from the trans state (0 ± 60°). However, ψi can visit a cis state (180°) for some of the glucopyranose units. This state is mostly responsible for the macroring distortion [31], [32] and [67]. At any temperature and due to larger substituent size, the NmβCD macroring is much less flexible than its XmβCDs partner [31]. Therefore, the distributions for φi and ψ torsional angles only get slightly wider upon increasing the temperature. The angles that describe the rotation around the ether type bonds that link the naphthyl moiety to the macroring (an example of the probability distributions depicted in Fig. S12, Supporting Information) change from the initial placements during the MD trajectory. However, this does not make substantial changes in the NmβCD initial full-open or open conformations.

The distributions of the distances between the center of mass of the naphthyl moiety and βCD macroring show single maxima at any temperature (Fig. S13, Supporting Information). The average of these distances only slightly increases with temperature. These distributions do not show any isosbestic points due the presence of a half-open/capped equilibrium, as was previously observed for the XmβCD partner [31]. Here, the NmβCD system is more rigid and, as stated before, no significant changes from the initial existing conformations were observed. This probably contribute to the large stabilization for (NmβCD)2.

Fig. 7 depicts the distribution of the angles between the 7-fold macro-ring CD axis and the 1Bb and 1La dipole transition moments obtained from the analysis of the MD trajectories in vacuum for the open (2) conformation (Fig. S11, Supporting Information) of NmβCD at two temperatures. Presumably, open conformations should be responsible for the ICD signal since it is unlikely that the naphthyl group interacts with the CD cavity in the full-open arrangement. The distribution presents a maximum at 89 ± 19° (26 ± 23°) for 1Bb (1La) transition at 350 K. At 600 K, due to the larger conformational sampling, the distributions are wider and show a maximum located at 99 ± 28° or even become bimodal for the angle with 1La (and 1Lb), with the maxima placed at 27 ± 24° and 107 ± 38°. The NMR experiments in deuterated chloroform, where only monomer exists, also point to a likely open conformation for NmβCD. The results of these distributions support the high intensity and positive sign of the 1Bb ICD band for NmβCD in non-polar solvents when the only species present in the medium is the monomer

and do not disagree with the sign and low intensity for the 1Lb (and 1La) band according to Kodaka's rules [57] and [58].

3.6.2. Dimerization of NmβCD to (NmβCD)2

Fig. 8 depicts the changes in the interaction energy for the dimer formation as a function of the distance along the y coordinate (d, Å) between the centers of both NmβCDs for different HH, HT and TT-type approaches, for the most stable full-open (1) and open (2) conformations (Supporting Information, named 1 and 2, Fig. S11,). Although quantitatively different, whatever the orientation of the approaching is, both conformations shown favourable interactions at the MBE. Nevertheless, dimers formed by HH approaching are the most energetically favourable. This conformation accords with the EC dual signal observed in the ICD spectrum in water, which requires the two relatively close naphthyl groups to interact. It also is in agreement with the recent calculations done before for other similar naphthalene-modified CDs, where the chromophore is linked to a single glucopyranose position positioned in the secondary rim [71]. Van der Waals attractive interactions are the most important contribution for any of the HH, HT and TT-type dimers whatever the initial full-open (1) or half-open (2) conformations were. However, differently to XmβCD self-association [31], the electrostatic contributions are also significant especially when both CDs approach HH oriented. These results agree with the experimental $\Delta H < 0$ which is the typical sign for attractive van der Waals and/or electrostatics interactions.

Table 2 collects some geometrical parameters and different interaction energy contributions that involve the naphthyl moieties of both CDs at the MBE. These contributions are favourable in most of the cases, except for TT approaching, where these interactions obviously do not exist. It is noticeable that the inter-naphthyl distance nearly fulfills the EC requirements for both (1) and (2) HH-type dimer conformations at the MBE. Superimposed in Fig. 8 are the MBE structures for both orientations of the HH, HT and TT (NmβCD)2 dimers that, once optimized again (0.5 kcal mol−1 Å−1), were used as starting structures for MD simulations.

Fig. 9 shows the history of the binding energies between NmβCD units for (NmβCD)2 dimers obtained from analysis of the 1.0 ns MD trajectories, as well as the distances between the center of mass of each NmβCD unit (Fig. S14 contains histories for other energetic interactions, Supporting Information). Table 2 also collects in parentheses the values of some of the parameters obtained for the minima binding energy structures achieved from the analysis of these trajectories. Again HH approaching is energetically more favourable than any other orientation. HT-dimers are stable during the whole 1 ns trajectory; TT-dimers, whatever the initial conformation was, dissociate reaching distances where CDs hardly interact. As collected in Table 2, the interaction energies for the MBE structures where naphthyl groups are involved, when they exist, were always more favourable when two NmβCD approach HH oriented.

Minima binding energy HH and HT-type structures for the (NmβCD)2 dimer obtained from the analysis of the 1 ns MD simulations are depicted in Fig. 10. This HH-open(2) dimer structure would agree with most of the experimental findings. For this arrangement the centers of both naphthalene rings are separated by 7.5 Å and whereas the naphthalene rings are nearly parallels and favourably interact, they are far away from a face-to-face stacked structure.

4. Conclusion

NMR, fluorescence, induced circular dichroism and molecular modelling techniques were used for studying the self-aggregation of NmβCD in water and organic solvents. Dimerization constants in water are three orders of magnitude larger than those previously obtained for similar β-cyclodextrin derivatives bearing double-linked xylynene moiety at the secondary ring, instead of the naphthyl one. Dimerization processes were both enthalpy and entropy favoured. The $\Delta H < 0$ values are quite similar to those obtained for the (XmβCD)2 formation. However, $\Delta S > 0$ in contrast with the negative value obtained for XmβCD (and also XmαCD and XmγCD [31] and [32]). This sign is attributed to the much higher loss of solvation order during dimerization in the case of the larger naphthyl groups compared with the benzene rings. NMR, ICD and fluorescence measurements indicate that dimerization takes place in high polar solvents. Similarly to that described for compounds in the xylylene-capped series [30], [31] and [32] a negative solubility coefficient for NmβCD was observed in water. This fact is compatible with a change in hydration status that is strongly dependent on temperature. Considering the highly hydrophobic character of the naphthalene platform, it is conceivable that this moiety is shielded from bulk water at low temperatures in the dimer form and becomes exposed when increasing the molecular mobility in the monomer at the highest temperatures.

MD calculations of NmβCD allow us to infer that the conformations possible for the appended groups are those that are open or full-open and the absence of any open ⇌ capped equilibrium. Theoretical results, in agreement with NMR spectra, the exciton coupling bisignal obtained in the ICD spectrum and quenching experiments in water, indicated that most stable and probable dimers are formed when both NmβCD approach head-to-head with both CDs placed in an open conformation. Nevertheless, calculations do not exclude the presence of head-to-tail ones. For these (NmβCD)2 structures the naphthyl moieties are relatively close to each other to couple their transition moments but without forming excimers and, although they do not penetrate inside the cavity of the neighbour CD, they may be relatively shielded from the solvent.

Acknowledgements

This work was supported by the Spanish MICINN (projects CTQ2008-03149/BQU and CTQ2010-15848/BQU), the EU (FEDER) and the Junta de Andalucía. M.J.G-A acknowledge FPU MICINN grants. FM and M.J.G-A acknowledge the assistance of M.L. Heijnen with the preparation of the manuscript.

References

[1] A. Douhal

Cyclodextrins Materials Photochemistry, Photophysics and Photobiology

Elsevier, Amsterdam (2006)

[2] H. Dodziuk

Cyclodextrins and Their Complexes

Wiley-VCH Verlag GmbH & Co. KGaA (2008)

[3] S. Li, W.C. Purdy

Cyclodextrins and their applications in analytical chemistry

Chem. Rev., 92 (1992), pp. 1457–1470

[4] E. Engeldinger, D. Armspach, D. Matt

Capped cyclodextrins

Chem. Rev., 103 (2003), pp. 4147–4173

[5] A.R. Khan, P. Forgo, K.J. Stine, V.T. D'Souza

Methods for selective modifications of cyclodextrins

Chem. Rev., 98 (1998), pp. 1977–1996

[6] H.H. Sigurdsson, E. Stefansson, E. Gudmundsdottir, T. Eysteinsson, M. Thorsteinsdottir, T. Loftsson

Cyclodextrin formulation of dorzolamide and its distribution in the eye after topical administration

J. Control. Release, 102 (2005), pp. 255–262

[7] R.I. Gelb, L.M. Schwartz

Complexation of adamantane–ammonium substrates by β-cyclodextrin and its O-methylated derivatives

J. Inclusion Phenom. Mol. Recognit. Chem., 7 (1989), pp. 537–543

[8] J. Shi, D.-S. Guo, F. Ding, Y. Liu

Unique regioselective binding of permethylated β-cyclodextrin with azobenzene derivatives

Eur. J. Org. Chem., 92 (2009), pp. 3–931

[9] Y. Liu, J. Shi, D.-S. Guo

Novel permethylated β-cyclodextrin derivatives appended with chromophores as efficient fluorescent sensors for the molecular recognition of bile salts

J. Org. Chem., 72 (2007), pp. 8227–8234

[10] T. Ogoshi, A. Harada

Chemical sensors based on cyclodextrin derivatives

Sensors, 8 (2008), pp. 4961–4982

[11] Y. Zhao, J. Gu, S.M. Chi, Y.C. Yang, H.Y. Zhu, Y.F. Wang, J.H. Liu, R. Huang

Aromatic diamino-bridged bis(β-cyclodextrin) as fluorescent sensor for the molecular recognition of bile salts

Bull. Korean Chem. Soc., 29 (2008), pp. 2119–2124

[12] X.-L. Chen, L.-B. Qu, T. Zhang, H. Liu, F. Yu, Y.-Z. Yu, Y.-F. Zhao

Direct observation of non-covalent complexes formed through phosphorylated flavonoid protein interaction by electrospray ionization mass spectrometry

Supramol. Chem., 16 (2004), pp. 67–75

[13] A. Ueno, T. Kuwabara, A. Nakamura, F. Toda

A modified cyclodextrin as a guest responsive color-change indicator

Nature, 356 (1992), pp. 136–137

[14] P.F. Wang, L. Jullien, B. Valeur, J.S. Filhol, J. Canceill, J.M. Lehn

Multichromophoric cyclodextrins. 5. Antenna-induced unimolecular photoreactions. Photoisomerization of a nitrone

New J. Chem., 20 (1996), pp. 895–907

[15] J.W. Park, H.E. Song, S.Y. Lee

Homo-dimerization and hetero-association of 6-O-(2-sulfonato-6-naphthyl)-β-cyclodextrin and 6-deoxy-(pyrene-1-carboxamido)-β-cyclodextrin

J. Org. Chem., 68 (2003), pp. 7071–7076

[16] S.R. McAlpine, M.A. Garcia-Garibay

Studies of naphthyl-substituted β-cyclodextrins. Self-aggregation and inclusion of external guests

J. Am. Chem. Soc., 120 (1998), pp. 4269–4275

[17] X.-M. Gao, L.-H. Tong, Y.-L. Zhang, A.-Y. Hao, Y. Inoue

Exciton coupling and binding behavior of β-cyclodextrin substituted by one 2-naphthoyl moiety

Tetrahedron Lett., 40 (1999), pp. 969–972

[18] X.-M. Gao, Y.-L. Zhang, L.-H. Tong, Y.-H. Ye, X.-Y. Ma, W.-S. Liu, Y. Inoue

Exciton coupling and complexation behavior of β-cyclodextrin naphthoate

J. Incl. Phenom. Macrocycl. Chem., 39 (2001), pp. 77–80

[19] K.K. Park, Y.S. Kim, S.Y. Lee, H.E. Song, J.W. Park

Preparation and self-inclusion properties of p-xylylenediamine-modified β-cyclodextrins: dependence on the side of modification

J. Chem. Soc., Perkin Trans., 2 (2001), pp. 2114–2118

[20] J.W. Park, S.Y. Lee, S.M. Kim

Efficient inclusion complexation and intra-complex excitation energy transfer between aromatic group-modified β-cyclodextrins and a hemicyanine dye

J. Photochem. Photobiol. A, 173 (2005), pp. 271–278

[21] F. Moriwaki, H. Kaneko, A. Ueno, T. Osa, F. Hamada, K. Murai

Excimer formation and induced-fit type of complexation of β-cyclodextrin capped by two naphthyl moieties

Bull. Chem. Soc. Jpn., 60 (1987), pp. 3619–3623

[22] A. Ueno, F. Moriwaki, T. Osa, F. Hamada, K. Murai

Fluorescence and circular dichroism studies on host-guest complexation of β-cyclodextrin bearing two 2-naphthyl moieties

Bull. Chem. Soc. Jpn., 59 (1986), pp. 465–470

[23] M.N. Berberan-Santos, J. Canceill, J.C. Brochon, L. Jullien, J.M. Lehn, J. Pouget, P. Tauc, B. Valeur

Multichromophoric cyclodextrins. 1. Synthesis of O-naphthoyl-β-cyclodextrins and investigation of excimer formation and energy hopping

J. Am. Chem. Soc., 114 (1992), pp. 6427–6436

[24] M.N. Berberan-Santos, J. Pouget, B. Valeur, J. Canceill, L. Jullien, J.M. Lehn

Multichromophoric cyclodextrins. 2. Inhomogeneous spectral broadening and directed energy hopping

J. Phys. Chem., 97 (1993), pp. 11376–11379

[25] M.N. Berberan-Santos, J. Canceill, E. Gratton, L. Jullien, J.-M. Lehn, P. So, J. Sutin, B. Valeur

Multichromophoric cyclodextrins. 3. Investigation of dynamics of energy hopping by frequency-domain fluorometry

J. Phys. Chem., 100 (1996), pp. 15–20

[26] S.R. McAlpine, M.A. Garcia-Garibay

Binding studies of adamantanecarboxylic acid and a naphthyl-bound β-cyclodextrin by variable temperature 1H NMR

J. Org. Chem., 61 (1996), pp. 8307–8309

[27] S.R. McAlpine, M.A. Garcia-Garibay

Inside–outside isomerism of β-cyclodextrin covalently linked with a naphthyl group

J. Am. Chem. Soc., 118 (1996), pp. 2750–2751

[28] J.W. Park, H.E. Song, S.Y. Lee

Face selectivity of inclusion complexation of viologens with β-cyclodextrin and 6-O-(2-sulfonato-6-naphthyl)-γ-cyclodextrin

J. Phys. Chem. B, 106 (2002), pp. 7186–7192

[29] J.W. Park, H.E. Song, S.Y. Lee

Facile dimerization and circular dichroism characteristics of 6-O-(2-sulfonato-6-naphthyl)-β-cyclodextrin

J. Phys. Chem. B, 106 (2002), pp. 5177–5183

[30] P. Balbuena, D. Lesur, M.J. González-Álvarez, F. Mendicuti, C. Ortiz Mellet, J.M. García Fernández

One-pot regioselective synthesis of 2I,3I-O-(o-xylylene)-capped cyclomalto-oligosaccharides: tailoring the topology and supramolecular properties of cyclodextrins

Chem. Commun., 327 (2007), pp. 0–3272

[31] M.J. González-Álvarez, P. Balbuena, C. Ortiz Mellet, J.M. García Fernández, F. Mendicuti

Study of the conformational and self-aggregation properties of 2I,3I-O-(o-xylylene)-per-O-Me-α- and -β-cyclodextrins by fluorescence and molecular modelling

J. Phys. Chem. B, 112 (2008), pp. 13717–13729

[32] M.J. González-Álvarez, J. Vicente, C. Ortiz Mellet, J.M. García Fernández, F. Mendicuti

Thermodynamics of the dimer formation of 2I,3I-O-(o-xylylene)-per-O-Me-β-cyclodextrin: fluorescence, molecular mechanics and molecular dynamics

J. Fluoresc., 19 (2009), pp. 975–988

[33] K. Uekama, T. Irie

D. Duchême (Ed.), Cyclodextrins and Their Industrial Uses, Edition Sante, Paris (1987), pp. 393–439

[34] K. Harata

X-ray structures of hexakis(2,6-di-O-methyl)-β-cyclodextrin in two crystal forms

Supramol. Chem., 5 (1995), pp. 231–236

[35] T. Steiner, F. Hirayama, W. Saenger

Topography of cyclodextrin inclusion complexes. Part 40. Crystal structures of hexakis-(2,6-di-O-methyl)-cyclomaltohexaose (dimethyl-β-cyclodextrin) crystallized from acetone, and crystallized from hot water

Carbohydr. Res., 296 (1996), pp. 69–82

[36] T. Steiner, W. Saenger

Topography of cyclodextrin inclusion complexes. Part 37. Crystal structure of anhydrous heptakis-(2,6-di-O-methyl) cyclomaltohepataose (dimethy-β-cyclodextrin)

Carbohydr. Res., 275 (1995), pp. 73–82

[37] T. Steiner, W. Saenger

Crystal structure of anhydrous hexakis(2,3,6-tri-O-methyl)cyclomaltohexaose (permethyl-β-cyclodextrin) grown from hot water and from cold NaCl solutions

Carbohydr. Res., 282 (1996), pp. 53–63

[38] T. Aree, I. Uson, B. Schulz, G. Reck, H. Hoier, G.M. Sheldrick, W. Saenger

Variation of a theme crystal structure with four octakis(2,3,6-tri-O-methyl)-β-cyclodextrin molecules hydrated differently by a total of 19.3 water

J. Am. Chem. Soc., 121 (1999), pp. 3321–3327

[39] T. Steiner, W. Saenger

Topography of cyclodextrin inclusion complexes. Part 43. Closure of the cavity in permethylated cyclodextrins through glucose inversion, flipping, and kinking

Angew. Chem., Int. Ed., 37 (1999), pp. 3404–3407

[40] T. Aree, H. Hoier, B. Schulz, G. Reck, W. Saenger

Novel type of thermostable channel clathrate hydrate formed by heptakis(2,6-di-O-methyl)-β-cyclodextrin·15H2O—a paradigm of the hydrophobic effect

Angew. Chem., Int. Ed., 39 (2000), pp. 897–899

[41] M.R. Caira, V.J. Griffith, L.R. Nassimbeni, O.B. van

Unusual 1C4 conformation of a methylglucose residue in crystalline permethyl-β-cyclodextrin monohydrate

J. Chem. Soc., Perkin Trans., 2 (1994), pp. 2071–2072

[42] The authors kindly thank Dr. C. Hunter for providing the titration isotherm curve fitting program. For detailed description of the fitting methods and equations, see:

(a) A.P. Bisson, C.A. Hunter, J.C. Morales, K. Young

Chem. Eur. J., 4 (1998), p. 845

(b) A.P. Bisson, F.J. Carver, D.S. Eggleston, R.C. Haltiwanger, C.A. Hunter, D.L. Livingston, J.F. McCabe, C. Rotger, A.E. Rowan

J. Am. Chem. Soc., 122 (2000), p. 8856

[43] N. Harting, G. Thielking, H.-F. Grutzmacher

Methoxymethyl group migration in bis(methoxymethyl)arene radical cations: a new outlook on the rearrangement of dialkylarene radical cations

Int. J. Mass Spectrom. Ion Processes, 167/168 (33) (1997), pp. 5–352

[44] M.J. González-Álvarez, A. Di Marino, F. Mendicuti

Fluorescence induced circular dichroism and molecular mechanics of 1-methyl naphthalenecarboxylate complexes with 2-hydroxypropyl cyclodextrins

J. Fluoresc., 19 (2009), pp. 449–462

[45] K. Harata, H. Uedaira

Circular dichroism spectra of the β-cyclodextrin complex with naphthalene derivatives

Bull. Chem. Soc. Jpn., 48 (1975), pp. 375–378

[46] J.R. Platt

Classification of spectra of cata-condensed hydrocarbons

J. Chem. Phys., 17 (1949), pp. 484–495

[47] D.V. O'Connor, W.R. Ware, J.C. Andre

Deconvolution of fluorescence decay curves. A critical comparison of techniques

J. Phys. Chem., 83 (1979), pp. 1333–1343

[48] F. Mendicuti

Applications of fluorescence techniques and modeling to the study of the complexation of chromophore-containing guests with cyclodextrins

Trends Phys. Chem., 11 (2006), pp. 61–77

[49] A. Di Marino, L. Rubio, F. Mendicuti

Fluorescence and molecular mechanics of 1-methyl naphthalenecarboxylate/cyclodextrin complexes in aqueous medium

J. Incl. Phenom. Macrocycl. Chem., 58 (2007), pp. 103–114

[50] A. Di Marino, F. Mendicuti

Fluorescence of the complexes of 2-methylnaphthoate and 2-hydroxypropyl-α, -β, and -γ-cyclodextrins in aqueous solution

Appl. Spectrosc., 56 (2002), pp. 1579–1587

[51] J.M. Madrid, F. Mendicuti

Thermodynamic parameters of the inclusion complexes of 2-methylnaphthoate and α- and β-cyclodextrins

Appl. Spectrosc., 51 (1997), pp. 1621–1627

[52] R.U. Lemieux

How water provides the impetus for molecular recognition in aqueous solution

Acc. Chem. Res., 29 (1996), pp. 373–380

[53] J.R. Lakowicz

Quenching of fluorescence

J.R. Lakowicz (Ed.), Principles of Fluorescence Spectroscopy, Springer, New York (2008), p. 280

[54] Y. Song, Y. Chen, Y. Liu

Switchable fluorescence behaviors of pyronine Y at different pH values upon complexation with biquinolino-bridged bis(β-cyclodextrin)

Photochem. Photobiol. A, 173 (2005), pp. 328–333

[55] T. Aoyagi, A. Nakamura, H. Ikeda, T. Ikeda, H. Mihara, A. Ueno

Alizarin yellow-modified β-cyclodextrin as a guest-responsive absorption change sensor

Anal. Chem., 69 (1997), pp. 659–663

[56] T. Kuwabara, H. Nakajima, M. Nanasawa, A. Ueno

Color change indicators for molecules using methyl red-modified cyclodextrins

Anal. Chem., 71 (1999), pp. 2844–2849

[57] M. Kodaka

Application of a general rule to induced circular dichroism of naphthalene derivatives complexed with cyclodextrins

J. Phys. Chem. A, 102 (1998), pp. 8101–8103

[58] M. Kodaka

Sign of circular dichroism induced by β-cyclodextrin

J. Phys. Chem., 95 (1991), pp. 2110–2112

[59] M. Kodaka

A general rule for circular dichroism induced by a chiral macrocycle

J. Am. Chem. Soc., 115 (1993), pp. 3702–3705

[60] M. Kodaka, T. Fukaya

Complex formation between heptylviologen and cyclodextrin

Bull. Chem. Soc. Jpn., 59 (1986), pp. 2032–2034

[61] M. Kodaka, T. Fukaya

Induced circular dichroism spectrum of a β-cyclodextrin complex with heptylviologen

Bull. Chem. Soc. Jpn., 62 (1989), pp. 1154–1157

[62] N. Berova, K. Nakanishi

Exciton chirality method: principles and applications

N. Berova, K. Nakanishi, R.W. Woody (Eds.), Circular Dichroism: Principles and Applications, Wiley-VCH (2000), pp. 337–382

[63] A. Douhal

Breaking, making, and twisting of chemical bonds in gas, liquid, and nanocavities

Acc. Chem. Res., 37 (2004), pp. 349–355

[64] SYBYL St. Louis, Missouri, USA, 2007.

[65] M. Clark, R.D. Cramer III, O.N. Van

Validation of the general purpose Tripos 5.2 force field

J. Comput. Chem., 10 (1989), pp. 982–1012

[66] M.J. Frisch et al.

MOPAC (AM1) included in the Gaussian 03 Package

Gaussian, Inc., Wallingford, CT (2004)

[67] J. Pozuelo, J.M. Madrid, F. Mendicuti, W.L. Mattice

Inclusion complexes of chain molecules with cycloamyloses. 1. Conformational analysis of the isolated cycloamyloses using molecular dynamics simulations

Comput. Theor. Polym. Sci., 6 (1996), pp. 125–134

[68] Y. Brunel, H. Faucher, D. Gagnaire, A. Rassat

Program of minimization of the empirical energy of a molecule by a simple method

Tetrahedron, 31 (1975), pp. 1075–1091

[69] W.H. Press, B.P. Flannery, S.A. Teukolski, W.T.E. Vetterling

Numerical Recipes: The Art of Scientific Computing

Cambridge University Press (1988)

[70] M. Blanco

Molecular silverware. I. General solutions to excluded volume constrained problems

J. Comput. Chem., 12 (1991), pp. 237–247 (2 plates)

[71] M.R. Gamieldien, I. Maestre, C. Jaime, K.J. Naidoo

Optimal configurations of capped β-cyclodextrin dimers in water maximise hydrophobic association

ChemPhysChem, 11 (2010), pp. 452–459

Figure and scheme captions

Figure 1. Absorption spectra for NmβCD in water dilute solution at 25 °C. Superimposed is the NmβCD structure showing the directions of the electronic transitions moments.

Figure 2. Emission spectra (λex = 295 nm) for NmβCD/water solutions in the 0–0.425 mM range of concentrations at 25 °C. Changes of the corrected fluorescence intensity with [NmβCD] at 25 °C are superimposed.

Figure 3. (Upper) Changes with the concentration of the monomer (■) and dimer () fractions (100 × fi) obtained from the different lifetime contributions ascribed to both species. (Bottom) Variation of the weighted average lifetime with the temperature for [NmβCD] = 0.00479 (■), 0.104 (●) and 0.394 mM (▲). (For interpretation of the references to color in this figure legend, the reader is referred to the web version of the article.)

Figure 4. Variation of the weighted average lifetime $\langle\tau\rangle$ with [NmβCD] water solutions at several temperatures: 5 °C (□); 15 °C (○); 25 °C (▵); 35 °C (▿); 45 °C (◊).

Figure 5. Changes in the lifetime averages ($\langle\tau\rangle$) (■) and the fractional dimer-to-monomer contribution ratios (□) with ε for fluorescence decay measurements performed on NmβCD 0.2 mM solutions of different solvents: water, methanol/water (20:80 and 50:50, v/v), methanol, ethanol and butanol at 25 °C. Idem upon adding AC up to reaching a 1.6 M concentration (× and +, respectively).

Figure 6. Absorption spectra () and circular dichroism () for NmβCD (0.2 mM in water) at 25 °C (upper); comparative circular dichroism spectra for NmβCD solution of a different polarity solvent at 25 °C ([NmβCD] ≈ 0.2 mM) (bottom). (For interpretation of the references to color in this figure legend, the reader is referred to the web version of the article.)

Figure 7. Probability distributions of the angles between the 7-fold CD axis and 1Bb (filled symbols) and 1La (open symbols) electronic transition moments for naphthyl group obtained from the analysis of the 10 ns MD trajectories performed on NmβCD half-open (2) conformation at 350 K (circles) and 600 K (squares).

Figure 8. Changes in the binding energies when a second NmβCD approaches a NmβCD (y coordinate in Å) by HH (□), HT (●) and TT (▵) orientations for the most stable full-open (1) and half-open (2) conformations. Superimposed are the MBE (NmβCD)2 structures.

Figure 9. Histories for CD–CD binding energies and center of mass distances for (NmβCD)2 dimers by HH (black), HT (light gray) and TT (gray) orientations starting from the minimized MBE structures obtained from MM calculations for the most stable full-open (1) (upper panels) and half-open (2) (bottom panels) conformations.

Figure 10. Minima binding energy structures HH-type (upper) and HT-type (bottom) for (NmβCD)2 dimer obtained from the analysis of the 1 ns MD simulations. Starting conformations were full-open (1) and open (2).

Scheme 1. Synthesis of, 2I,3I-O-(1,8-naphthalene)-per-O-methyl-β-cyclodextrin (NmβCD) from 2I,3I-O-(o-xylylene)-per-O-methyl-β-cyclodextrin (XmCDs).

Table 1

Table 1. Association constants K_D, $\tau_{Nm\beta CD}$ and τ(NmβCD)2 parameters obtained from analysis of decay profiles at different [N*m*βCD] and temperatures.

T **(°C)**	10^{-3} K_D (M^{-1})	$\tau_{Nm\beta CD}$	**τ(NmβCD)2**
5	216 ± 202	26.5 ± 1.6	32.4 ± 0.2
15	137 ± 127	26.1 ± 1.2	30.8 ± 0.2
25	92 ± 58	25.5 ± 0.6	29.8 ± 0.2
35	78 ± 44	24.0 ± 0.6	28.9 ± 0.2
45	69 ± 34	22.8 ± 0.6	27.8 ± 0.2

Table 2

Table 2. Binding energy and other contributions (kJ mol^{-1}), as well as, several geometrical parameters for the structures 1 and 2 of *MBE* for N*m*βCD by *HH*, *HT* and *TT* approaching obtained by MM calculations. In parentheses are the structures for minima binding energy obtained from the analysis of the 1 ns MD trajectories in the presence of water as a solvent.

Parameter	***HH*(1)**	***HT*(1)**	***TT*(1)**	***HH*(2)**	***HT*(2)**	***TT*(2)**
Distance CD–CD (Å)	9.6 (9.8)	10.1 (10.0)	13.8 (13.3)	8.7 (9.6)	11.0 (11.2)	13.3 (13.9)
Distance N1–N2 (Å)	4.9 (5.1)	8.5 (10.3)	21.8 (19.5)	6.8 (7.5)	10.6 (10.4)	22.5 (24.0)
θ (°)	11.2 (18.2)	0.1 (−133.4)	13.4 (26.4)	40.3 (25.6)	0.3 (−171.5)	19.3 (14.7)
$E_{binding}$ (kJ mol^{-1})	−64.2 (−108.9)	−31.4 (−67.2)	−17.8 (−31.8)	−55.0 (−93.7)	−45.8 (−51.6)	−21.7 (−25.8)
Electrostatics	−11.0 (−17.5)	−2.8 (−4.4)	+5.0 (+4.3)	−20.8 (−11.1)	−3.3 (+5.4)	2.0 (−1.3)
van der Waals	−53.1 (−91.4)	−28.5 (−62.8)	−22.9 (−36.1)	−34.3 (−82.7)	−42.5 (−57.0)	−27.0 (−24.5)
E_{inter} N2–N*m*CD1	−49.9 (−44.5)	−0.2 (−6.9)	0 (0)	−37.3 (−17.3)	−4.3 (−13.5)	0 (0)
E_{inter} N1–N*m*CD2	−41.8 (−61.0)	−12.1 (−5.3)	0 (0)	−18.5 (−23.4)	−23.6 (−2.2)	0 (0)
E_{inter} N1–N2	−29.4 (−36.4)	+0.6 (−1.0)	0 (0)	−8.4 (−12.3)	−3.5 (−3.8)	0 (0)

Figure 1

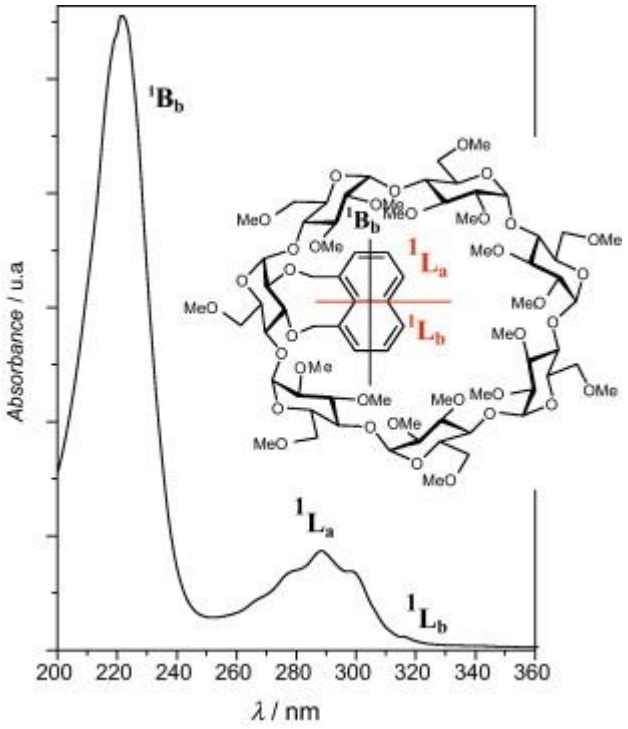
Absorbance / u.a
λ / nm
200
220
240
260
280
300
320
340
360
^1B_b
^1L_a
^1L_b
OMe
MeO

Figure 2

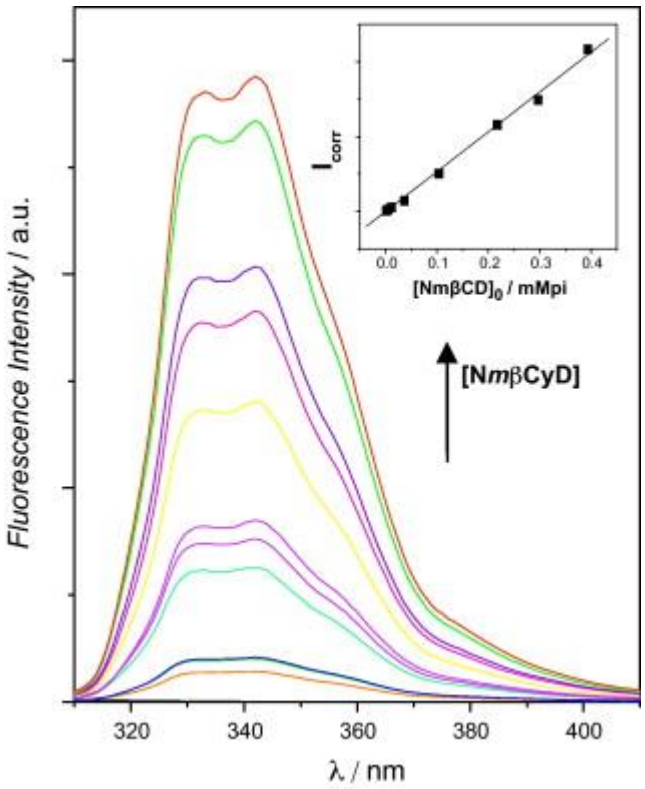
Fluorescence Intensity / a.u.
320
340
360
380
400
λ / nm
I corr
0.0
0.1
0.2
0.3
0.4
[NmβCD]0 / mMpi
[NmβCyD]

Figure 3

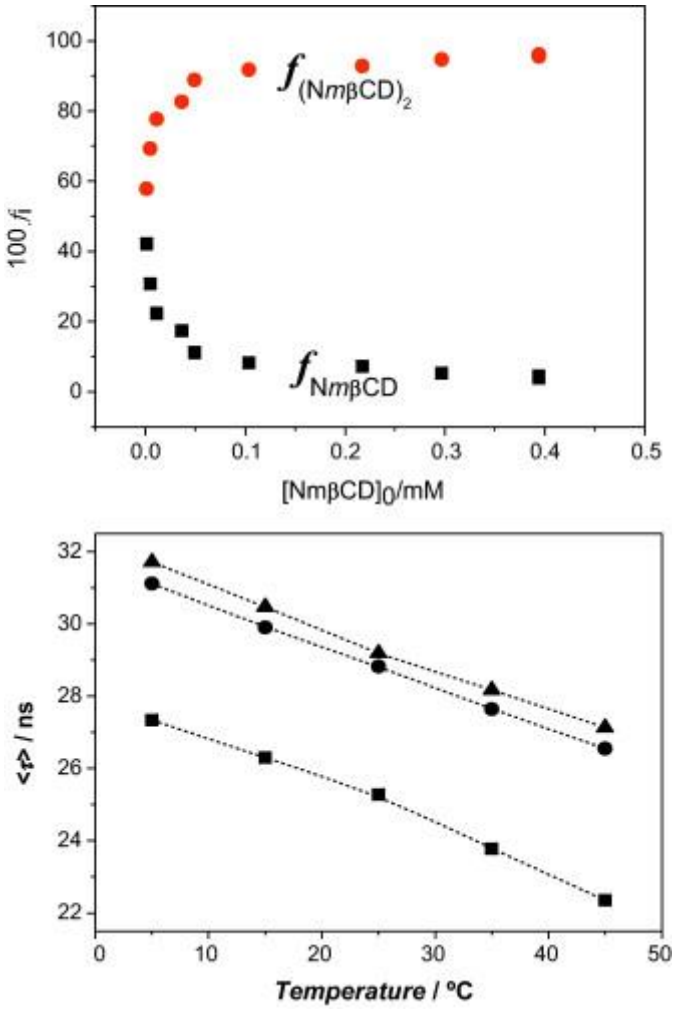
100
80
60
40
20
0
100 fi
$f_{(N m\beta CD)_2}$
$f_{N m\beta CD}$
0.0
0.1
0.2
0.3
0.4
0.5
[NmβCD]0/mM
32
30
28
26
24
22
<τ> / ns
0
10
20
30
40
50
Temperature / °C

Figure 4

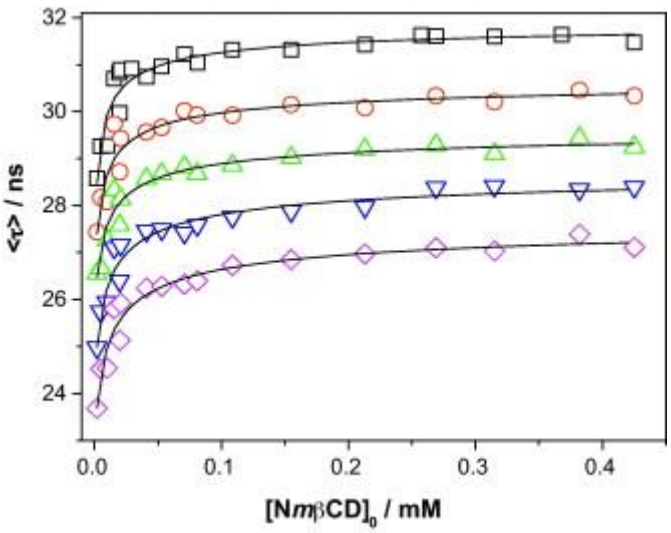

Figure 5

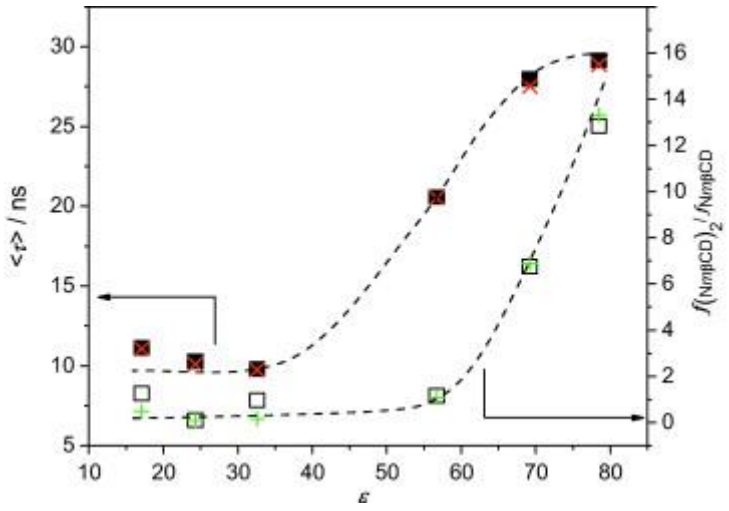
<τ> / ns
$f_{(NmβCD)_2}$ / $f_{NmβCD}$
ε
30
25
20
15
10
5
16
14
12
10
8
6
4
2
0
10
20
30
40
50
60
70
80

Figure 6

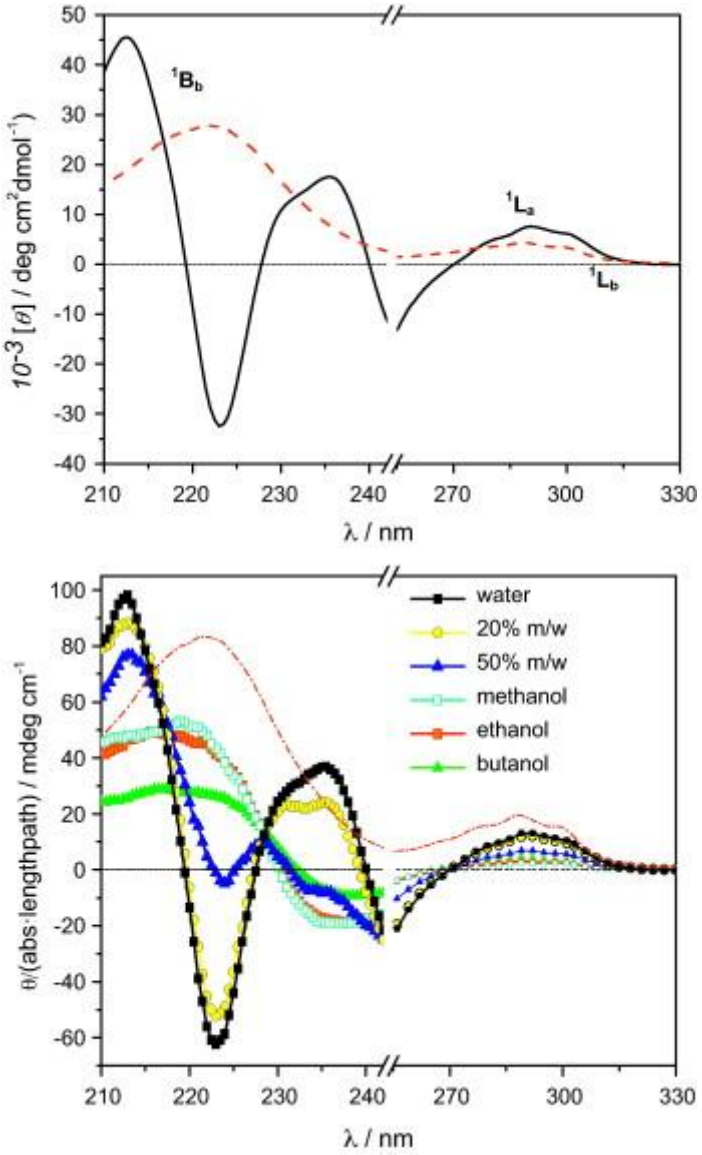
^1B_b
^1L_a
^1L_b
10^{-3} [θ] / deg cm^{2}dmol^{-1})
λ / nm
water
20% m/w
50% m/w
methanol
ethanol
butanol
θ/(abs·lengthpath) / mdeg cm^{-1}
λ / nm

Figure 7

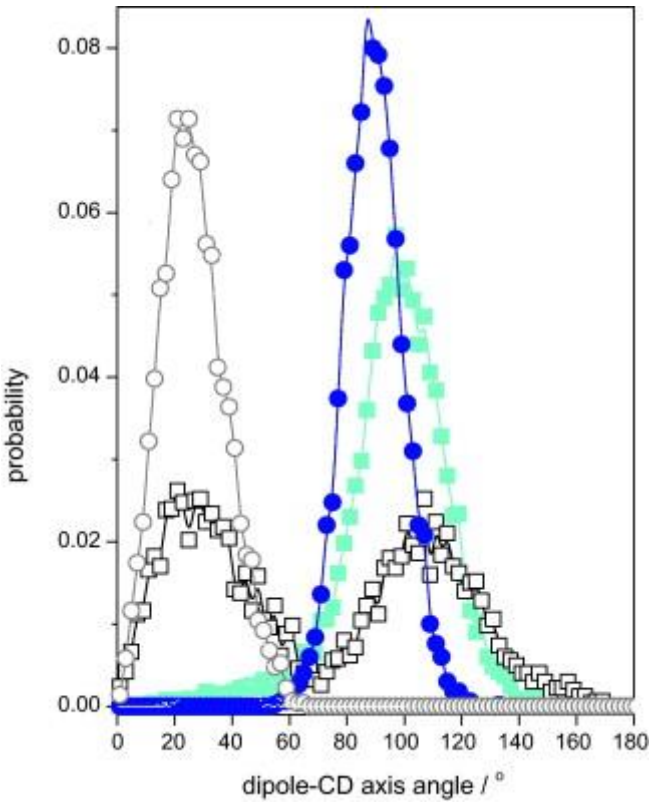
probability
0.08
0.06
0.04
0.02
0.00
0
20
40
60
80
100
120
140
160
180
dipole-CD axis angle / °

Figure 8

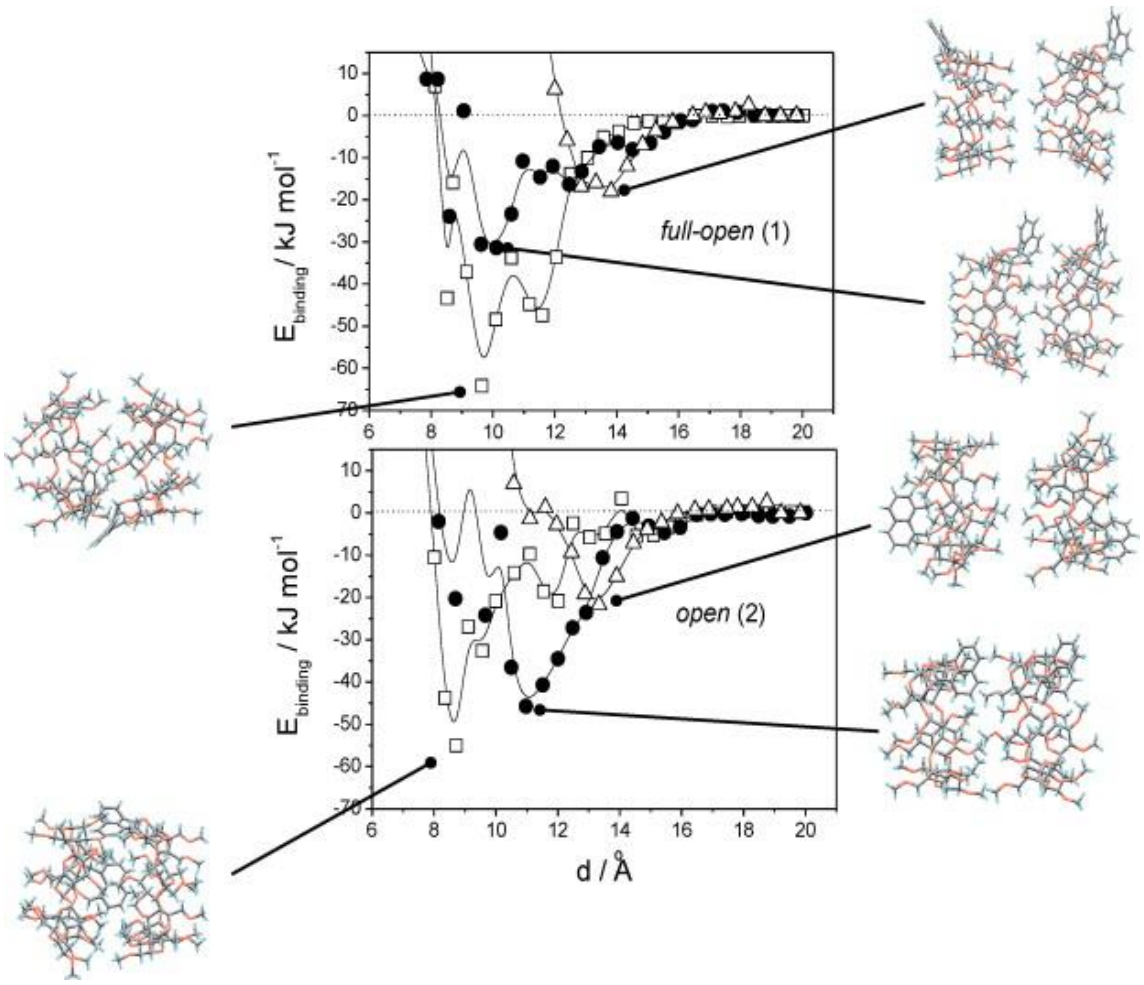

Figure 9

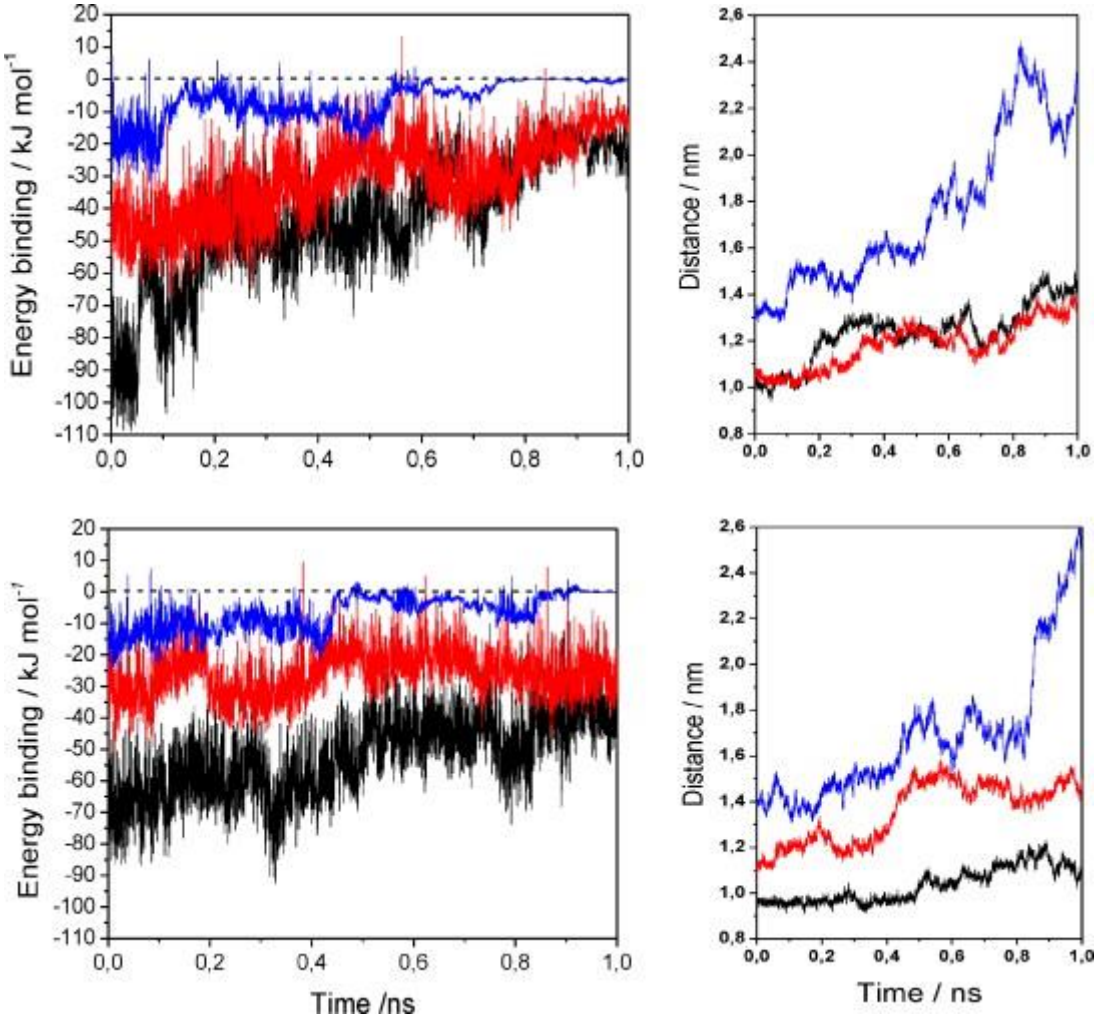
Energy binding / kJ mol-1
Distance / nm
Energy binding / kJ mol-1
Distance / nm
Time /ns
Time / ns

Figure 10

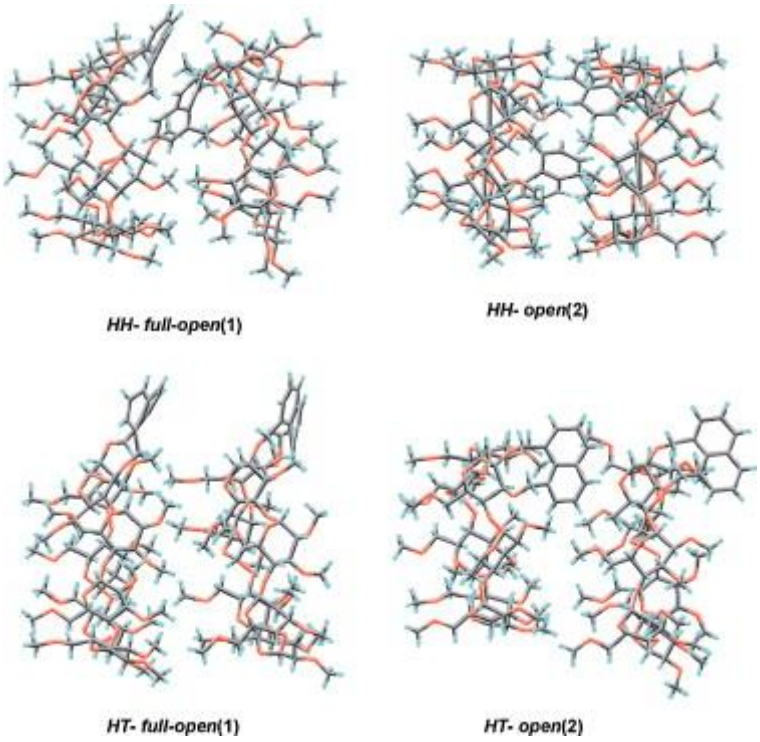

Scheme 1

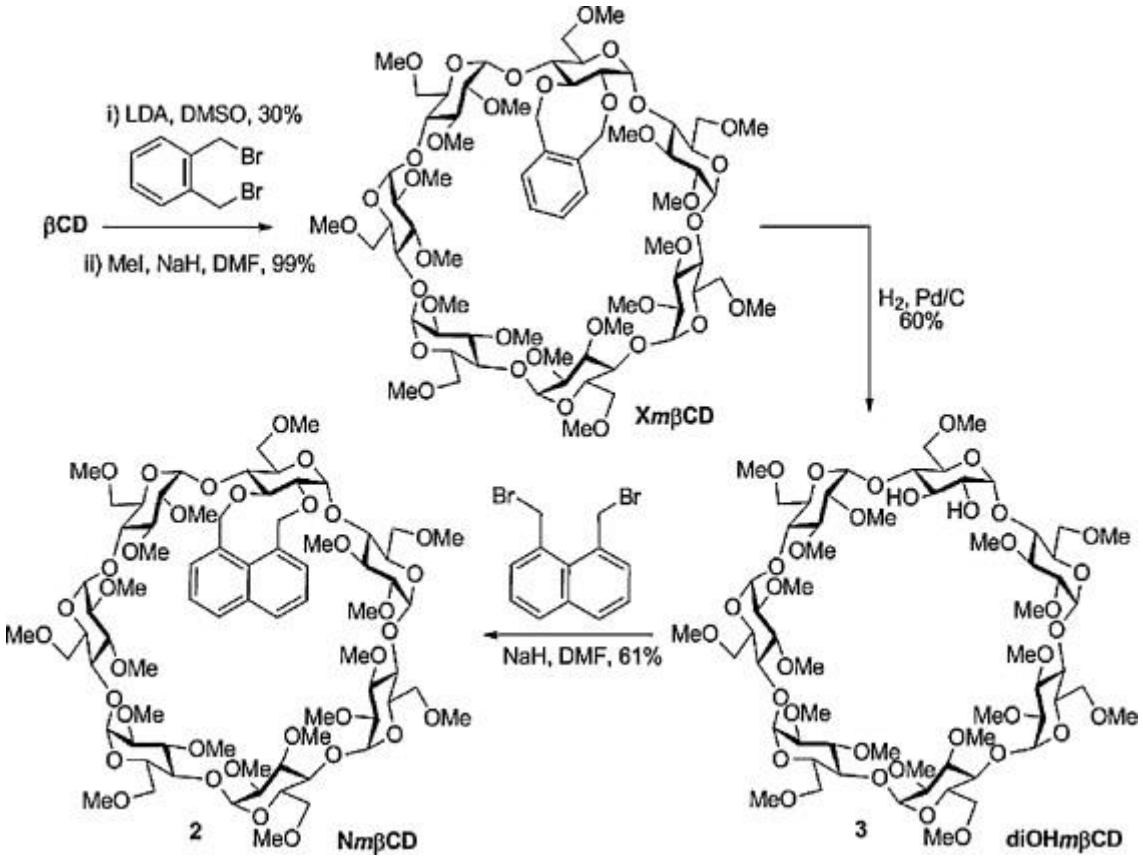
i) LDA, DMSO, 30%
Br
Br
βCD
ii) MeI, NaH, DMF, 99%
XmβCD
H2, Pd/C
60%
diOHmβCD
3
NaH, DMF, 61%
Br
Br
NmβCD
2